# Structural and electrical properties of laser-crystallized nanocrystalline Ge films and nanocrystalline Ge/SiN$_x$ multilayers*

Li Cong(李 悰), Xu Jun(徐 骏)†, Li Wei(李 伟), Jiang Xiao-Fan(江小帆), Sun Sheng-Hua(孙胜华), Xu Ling(徐 岭), and Chen Kun-Ji(陈坤基)

*National Laboratory of Solid State Microstructures, School of Physics, and School of Electronic Science and Engineering, Nanjing University, Nanjing* 210093, *China*

(Received 21 February 2013; revised manuscript received 19 April 2013)

Nanocrystalline Ge (nc-Ge) single layers and nc-Ge/SiN$_x$ multilayers are prepared by laser annealing amorphous Ge (a-Ge) films and a-Ge/SiN$_x$ multilayers. The microstructures as well as the electrical properties of laser-crystallized samples are systematically studied by using various techniques. It is found that the optical band gap of nc-Ge film is reduced compared with its amorphous counterpart. The formed nc-Ge film is of p-type, and the dark conductivity is enhanced by 6 orders for an nc-Ge single layer and 4 orders for a multilayer. It is suggested that the carrier transport mechanism is dominant by the thermally activation process via the nanocrystal, which is different from the thermally annealed nc-Ge sample at an intermediate temperature. The carrier mobility of nc-Ge film can reach as high as about 39.4 cm$^2$·V$^{-1}$·s$^{-1}$, which indicates their potential applications in future nano-devices.

**Keywords:** nanocrystalline Ge, microstructure, carrier transport, mobility

**PACS:** 72.20.Ee, 73.63.–b, 78.20.–e, 78.67.Bf **DOI:** 10.1088/1674-1056/22/10/107201

## 1. Introduction

Recently, the fabrication of nanocrystalline Si- and Ge-based films have aroused increasing the interest of researchers because they can be potentially used in many kinds of devices such as nonvolatile flash memories, solar cells, light emitters, and photodetectors due to their novel physical properties.[1–6] Compared with Si, Ge has a smaller effective mass and larger dielectric constant. Therefore, it can facilitate the modulation of its electronic structure to meet different applications by controlling the grain size of nanocrystalline Ge (nc-Ge). Furthermore, Ge has a larger electron and hole mobility, which can be used to fabricate the Ge-based thin film transistor (TFT) with good device performance.[7] It was also reported that the programming/erasing efficiency of poly-Si nonvolatile memories can be obviously improved by using nc-Ge as a charge trapping layer.[8]

Usually, nc-Ge films can be formed by the thermal annealing (TA) of amorphous Ge (a-Ge). The a-Ge films can be crystallized when the annealing temperature is about 400 °C.[9,10] In order to lower the annealing temperature, metal-induced crystallization was used and the crystallization temperature could reach as low as 165 °C.[11] However, unintentional doping took place and undesired impurities existed.[12] Alternatively, laser annealing (LA), as an inexpensive and rapid processing technique, was developed. A pulse laser was used to melt the films locally in a short time and then let them cool down rapidly.[13] Unlike thermal annealing, it provides local modification of surface with a low thermal budget.[14] Salihoglu *et al.*[15] reported on the crystallization of Ge in SiO$_x$ matrix by using a Ti:sapphire femtosecond pulse laser. The structural changes have been studied as a function of laser irradiation duration. Watakabe *et al.*[16] used a XeCl pulse laser to prepare crystallized Ge films with a conductivity of 3.5 S·cm$^{-1}$ for the application of high mobility Ge TFT. From the viewpoint of device applications, it is necessary to further understand the laser crystallization of a-Ge films to form nc-Ge and study the carrier transport process of nc-Ge films systematically.

In our previous work,[9] we prepared nc-Ge films on quartz substrates by thermal annealing and studied the structural, optical, and electrical properties. It was found that nc-Ge films with sizes of 10 nm–30 nm could form at the moderate annealing temperatures (450 °C–600 °C), whose hole mobility could reach as high as 211 cm$^2$·V$^{-1}$·s$^{-1}$. The Ge films showed p-type behaviors and the conduction mechanism was dominated by the transport process between Ge nanocrystals. In the present paper, a single layer (SL) of hydrogenated amorphous germanium (a-Ge:H) is prepared in a conventional plasma-enhanced chemical vapor deposition (PECVD) system. KrF excimer laser crystallization is used to form nc-Ge films on quartz substrates. The microstructural evolution from amorphous to nanocrystalline phase and optical and electrical properties are systematically studied. The differences between laser annealed and the thermally annealed nc-Ge films[9] are

*Project supported by the National Basic Research Program of China (Grant No. 2013CB632101), the National Natural Science Foundation of China (Grant Nos. 11274155 and 61036001), and Priority Academic Program Development of Jiangsu Higher Education Institutions, Jiangsu Province, China.

†Corresponding author. E-mail: junxu@nju.edu.cn

© 2013 Chinese Physical Society and IOP Publishing Ltd 

compared. It is found that for an nc-Ge single layer, the room temperature conductivity and the hole mobility can reach as high as 16.0 $S\cdot cm^{-1}$ and 39.4 $cm^2\cdot V^{-1}\cdot s^{-1}$, respectively. In order to achieve more controllable nc-Ge materials, we further prepare a-Ge:H/ $SiN_x$ multilayers (MLs) and laser crystallization is carried out to obtain nc-Ge/$SiN_x$ MLs. The carrier transport properties are also studied and compared with those of single layered samples. It is found that both the crystallinity and the film structures can influence the electrical properties and the transport mechanism in multilayered sample is also discussed.

## 2. Experiments

An a-Ge:H single layer with a thickness of 160 nm was deposited on quartz substrate in a conventional PECVD system by using a gas mixture of $H_2$ and $GeH_4$. During the deposition, the gas flow of $GeH_4$, the RF power, and the substrate temperature were kept at 2 sccm (standard-state cubic centimeter per minute), 30 W, and 250 °C, respectively.

An a-Ge:H/$SiN_x$ multilayer was prepared by alternatively depositing amorphous silicon nitride (a-$SiN_x$) and a-Ge:H with 25 periods followed by an a-$SiN_x$ capping layer. $H_2$ and a pure $GeH_4$ (2 sccm) gas mixture was used to prepare a-Ge:H sublayer, while $SiH_4$ (4 sccm), $NH_3$ (20 sccm), and $H_2$ were mixed to deposit an a-$SiN_x$ sublayer. The Si/N ratio in amorphous $SiN_x$ film is 0.93, which was estimated by X-ray photoelectron spectroscopy. The thickness of $SiN_x$ layer was constant (6 nm), whereas that of Ge sub-layer was varied from 10 nm to 6 nm to 4 nm sequentially.

After deposition, the samples were individually irradiated by a KrF excimer laser (248 nm, 30 ns) under one shot. The laser beam was modulated by a homogenizer so that the laser energy was distributed uniformly in a spot of 1 cm×1 cm. The laser fluence used is 100 mJ/$cm^2$–260 mJ/$cm^2$ for a single layer and 170 mJ/$cm^2$ for a multilayer.

The microstructures of Ge films were characterized by Fourier transform infrared spectroscopy (FTIR), Raman scattering spectroscopy, and transmission electron microscopy (TEM). Raman signals were detected using a Jobin–Yvon HR800 system at room temperature and excited by an $Ar^+$ laser (488 nm) in a backscattering geometry. The optical absorption characteristics of the films were obtained by measuring the reflectance and transmittance spectra. The temperature-dependent dark conductivity were measured in a vacuum chamber by evaporation coplanar Al electrode on front surface of film. Before the measurements, all samples were heated at 150 °C for 30 min to remove the absorbates of films and the test temperature ranges from 423 K to room temperature. The conduction type, carrier concentration, and mobility of the sample were measured using a Hall system with the Van der Pauw method at room temperature.

## 3. Results and discussion

### 3.1. Laser crystallization of a-Ge:H a single layer

Figure 1(a) shows the Raman spectra of samples before and after laser annealing under some different laser fluences. For the as-grown sample, only a hump around 275 $cm^{-1}$ can be identified, revealing its amorphous nature. After laser irradiation under 100 mJ/$cm^2$, there appears a peak centred at 298 $cm^{-1}$, which corresponds to the TO mode of the crystallized Ge–Ge phase[17] due to the partial crystallization of a-Ge:H film. With the further increase of laser fluence, the Raman peak is slightly blue-shifted toward that of bulk Ge, while the full width at half maximum (FWHM) narrows from 7.5 $cm^{-1}$ to 6.2 $cm^{-1}$ as shown in Fig. 1(b). It is suggested that the crystallinity improves and the average grain size increases with laser fluence increasing. To quantify the degree of crystallinity of nc-Ge film, the spectrum was decomposed into two Gaussian bands: a crystalline band close to 300 $cm^{-1}$ and an amorphous band at 275 $cm^{-1}$. The inset of Fig. 1(a) shows the decomposition result of nc-Ge sample. The crystallinity $X_C$ can be evaluated as[18]

$$X_C = I_C/(I_C + I_a), \tag{1}$$

where $I_c$ and $I_a$ denote the integrated intensities of the crystalline and amorphous phase, respectively. As shown in the inset of Fig. 1(b), the crystallinity increases from 46% to 60% with laser fluence increasing from 100 mJ/$cm^2$ to 260 mJ/$cm^2$.

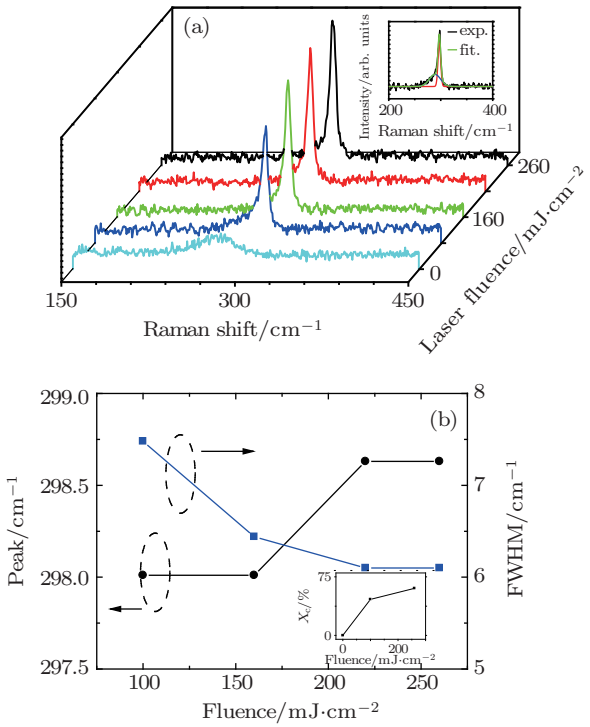



**Fig. 1.** (color online) (a) Raman spectra of films before and after annealing under some different laser fluences, and (b) peak positions and full widths at half maximum (FWHMs) of Raman spectra shown in Fig. 1(a). The insets of Figs. 1(a) and 1(b) show the decomposition of Raman spectra and the corresponding crystallinity, respectively.

It means that the a-Ge:H films can be nanocrystallized at quite a low laser fluence compared with the case of a-Si:H films,[19] which may result from the weak bonding strengths of Ge–Ge and Ge–H bonds compared with those of Si–Si and Si–H bonds, respectively.

The values of absorption coefficient ($\alpha$) of the samples before and after laser crystallization were obtained by measuring the reflectance and transmittance spectra. As shown in Fig. 2, the values of $\alpha$ exceed $10^3$ cm$^{-1}$ for all samples when the photon energy is higher than 1 eV, while the absorption edges are red-shifted after laser crystallization. Based on the absorption spectra, the values of optical band gap ($E_{\rm opt}$) of a-Ge:H[20] and nc-Ge films[21] can be deduced, which is shown in Table 1. It is found that the optical band gap decreases from 1.08 eV for as-grown a-Ge:H film to 0.91 eV for nc-Ge film due to the formation of Ge nanocrystals. With laser fluence further increasing to 260 mJ/cm$^2$, $E_{\rm opt}$ decreases to 0.87 eV, which can be ascribed to the increase of grain size and crystallinity as revealed by Raman spectra.

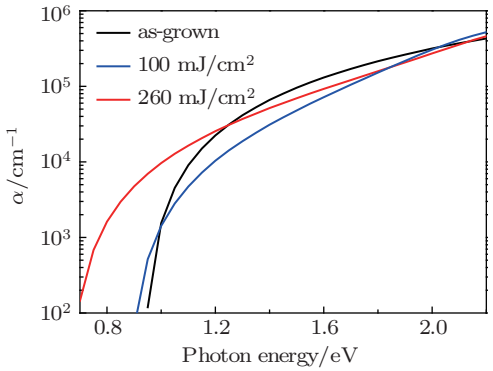



**Fig. 2.** (color online) Absorption coefficient spectra for as-grown and laser-crystallized a-Ge:H films.

It is interesting to investigate the influence of laser fluence on the carrier transport process in nc-Ge film. Here, we measured the temperature-dependent dark conductivities ($\sigma$) (from about 300 K to 423 K) by using coplanar configurations as shown in the inset of Fig. 3(a). As we can see, the conductivity of amorphous Ge sample increases from $9.2\times10^{-5}$ S·cm$^{-1}$ to $8.1\times10^{-3}$ S·cm$^{-1}$ as temperature increases from room temperature to 423 K. As for the nc-Ge films obtained by laser crystallization under 100 mJ/cm$^2$ and 260 mJ/cm$^2$, respectively, there are only small variations for conductivities in the measured temperature range. Moreover, the room temperature conductivity ($\sigma_{\rm RT}$) of nc-Ge film obtained under a laser fluence of 100 mJ/cm$^2$ is increased by 5 orders of magnitude compared with that of a-Ge:H sample as shown in Fig. 3(b). With fluence increasing to 260 mJ/cm$^2$, $\sigma_{\rm RT}$ is further enhanced by one order of magnitude ($\sim$ 16.0 S·cm$^{-1}$), which is much higher than those reported previously[16,22,23] but a little lower than the value of thermally annealed samples reported in our previous work.[9] The improvement of dark conductivity for laser-crystallized nc-Ge film can be attributed to the following factors: the reduction of optical band gap and the formation of nanocrystalline Ge phase. With the decrease of $E_{\rm opt}$, more carriers can be generated to make contributions to conductivity. On the other hand, after the formation of Ge nanocrystals, the carrier transport process is changed compared with that in amorphous sample. The corresponding carrier mobility can be improved which also results in the increase in conductivity.

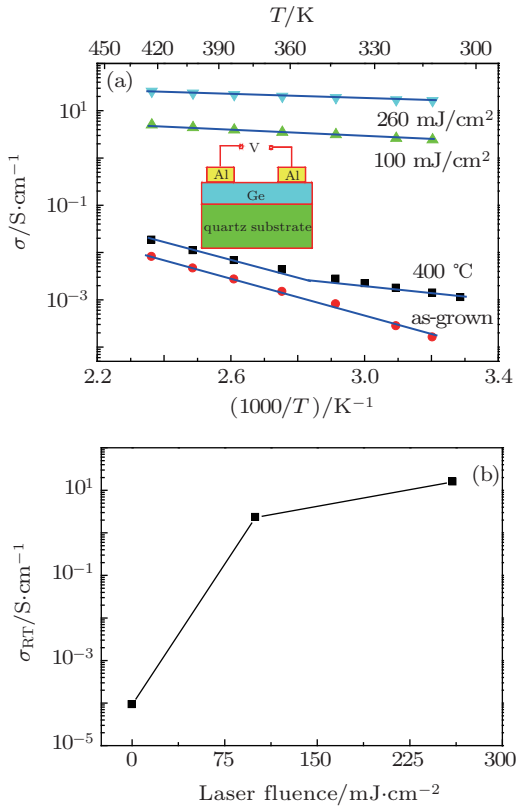



**Fig. 3.** (color online) (a) Temperature-dependent dark conductivities, and (b) room temperature dark conductivities before and after laser crystallization under 100 mJ/cm$^2$–260 mJ/cm$^2$. The inset of Fig. 3(a) is the sketch of conductivity tests.

In order to further understand the mechanism of the carrier transport process in nc-Ge film, we plot the temperature-dependent dark conductivity according to the Arrhenius relationship,

$$\sigma = \sigma_0 \exp(-E_{\rm a}/k_{\rm B}T), \tag{2}$$

where $\sigma_0$, $k_{\rm B}$, $E_{\rm a}$, and $T$ are the pre-factor of conductivity, Boltzmann constant, conduction activation energy, and absolute temperature, respectively. As shown in Fig. 3(a), a good linear relationship can be achieved for our samples, which strongly indicates that the thermally activation conduction is dominated in the transport process. The activation energies are deduced and given in Table 1. It is found that $E_{\rm a}$ of the as-grown sample is about 0.35 eV. Considering the fact that

the optical band gap of a-Ge:H is 1.08 eV, it is found that $E_a$ is smaller than $E_{opt}/2$ just like the case of a-Si:H.[24] Usually, at a temperature range from room temperature to 423 K, the carrier conduction is ascribed to the transport in extended states, which means $E_a = E_C - E_F$ or $E_a = E_F - E_V$. Here $E_C$, $E_F$, and $E_V$ denote electron mobility edge, Fermi level, and hole mobility edge, respectively. In some references[16,22,25] amorphous Ge films were reported to exhibit n-type behaviors, but in our case, the Hall measurements indicate that a-Ge:H films are of p-type (which will be discussed below). Therefore, $E_a$ equals the energy difference between Fermi level and valence band edge ($E_a = E_F - E_V$). It indicates that the Fermi level in a-Ge:H film is located the 0.35 eV above the valence band edge. After the formation of Ge nanocrystal by laser annealing, the corresponding activation energy $E_a$ drops drastically to 0.04 eV–0.06 eV. The quite a small activation energy means that more carriers (mainly holes in our case) can be easily thermally generated to contribute to the conduction process.

**Table 1.** Optical band gaps and activation energies of samples.

| samples | Ge SL | | | Ge/$SiN_x$ MLs (170 mJ/cm$^2$) | | |
|---|---|---|---|---|---|---|
| | as-grown | 100/(mJ/cm$^2$) | 260/(mJ/cm$^2$) | 4 nm/6 nm | 6 nm/6 nm | 10 nm/6 nm |
| $E_{opt}$ /eV | 1.08 | 0.91 | 0.87 | 0.83 | 0.77 | 0.70 |
| $E_a$ /eV | 0.35 | 0.06 | 0.04 | 0.08 | 0.08 | 0.04 |

$E_{opt}$: optical band gap; $E_a$: conduction activation energy

Hall measurements were also carried out for sample after laser annealing under 260 mJ/cm$^2$. According to the Hall measurement results, the nc-Ge sample in our case is of p-type. Such a p-type result was also found in nc-Ge embedded in $SiO_2$ matrix,[23] poly-Ge,[26] and Ge nanowires,[27] which may be due to hole accumulation induced by the surface states. The surface states pin the Fermi level near the valence band, hence causing the p-type behavior. In our case, the activation energy for hole conduction ($E_a \approx |E_F - E_V|$) is very small, indicating that $E_F$ is pinned very close to $E_V$ and even enters into the valence bands. Such a small activation energy also causes only a small variation of conductivity with temperature varying from 423 K to room temperature. Based on the Hall measurements, the hole concentration $p$ of nc-Ge is on the order of $10^{18}$ cm$^{-3}$, which is obviously increased by 7 orders of magnitude compared with that of a-Ge:H ($\sim 10^{11}$ cm$^{-3}$). Such a high carrier concentration results in a surprisingly high conductivity of nc-Ge. It is also worthy to note that after laser crystallization, the Hall mobility increases from 0.11 cm$^2\cdot$V$^{-1}\cdot$s$^{-1}$ for a-Ge:H film to 39.4 cm$^2\cdot$V$^{-1}\cdot$s$^{-1}$ for nc-Ge film, which is much higher than those reported in previous work.[22,23] Tsao *et al.*[22] reported on the crystallized Ge film with a mobility of a few cm$^2\cdot$V$^{-1}\cdot$s$^{-1}$, deposited by RF sputtering at a relatively high power (150 W) and a substrate temperature of 400 °C, showing that the post-treatment is helpful for improving the carrier mobility of nc-Ge. It was also reported in Ref. [23] that the mobility of nanocrystalline Ge dispersed in $SiO_2$ matrix was about 2.3 cm$^2\cdot$V$^{-1}\cdot$s$^{-1}$ after annealing at 800 °C. In our case, we used a KrF pulsed excimer laser to crystallize a-Ge films to obtain the nc-Ge. The laser irradiation can cause quite a high temperature ($>$ 1000 °C),[28–30] which is helpful for improving the crystallinity as well as the mobility. Therefore, the carrier mobility of the obtained nc-Ge film is obviously increased. On the other hand, the Ge nanocrystals in our sample are dispersed in a-Ge rather than in a $SiO_2$ matrix, and hence the corresponding scattering barrier is much weaker than that of nc-Ge in $SiO_2$, which is also beneficial to the improvement on mobility.

In our previous work,[9] we found that the well-crystallized nc-Ge films can be prepared by thermal annealing at temperatures above 450 °C, and the corresponding transport process is determined by the conduction through Ge nanocrystals as discussed above. As to the films annealed at intermediated annealing temperatures (350 °C and 400 °C), however, the conduction shows dual conduction activation processes. As shown in Fig. 3(a), the $\ln\sigma$–$T^{-1}$ plot of nc-Ge film annealed at 400 °C can be divided into two regions like in the case of a-Si:H.[24] The dual conduction process was ascribed to the effusion of hydrogen during the thermal annealing. After hydrogen effused out of the films, the sample becomes more defective and localized states are formed, which results in a new conduction channel via the localized states besides the extended states.

For the nc-Ge films obtained by laser crystallization, only a single conduction activation process was observed. It is ascribed to the incomplete effusion of hydrogen in the laser crystallization process in a very short time. In order to confirm this point, the bonding configurations of samples were investigated by FTIR. As shown in Fig. 4, an absorption band around 570 cm$^{-1}$ can be well identified in the as-grown sample, which can be ascribed to the Ge–H wagging mode. Although it becomes a little bit weak, this band still exists in the sample after laser annealing under a fluence of 260 mJ/cm$^2$. It indicates that some of the hydrogen atoms remain in the laser-crystallized film accompanied with the formation of nc-Ge, which can well passivate the defects states in nc-Ge film. However, for the sample annealed at 350 °C, the absorption

band becomes very weak, which manifests that a great number of Ge–H bonds have been broken in the post-thermal annealing process. As annealing temperature increases to 450 °C, this band completely disappears in the film. The effusion of hydrogen atoms may induce some localized defect states in the thermally annealed sample. Therefore, the carriers in the thermally annealed sample at an intermediate temperature can transport via both extended states in a high temperature region of 423 K–360 K and localized states by a hopping process in a low temperature region of 360 K–300 K,[9] whereas there is only a conduction channel through extended states in the laser-annealed nc-Ge films.

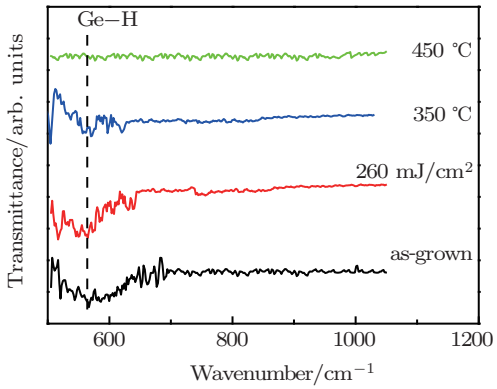



**Fig. 4.** (color online) FTIR spectra of as-grown a-Ge:H film, laser annealed nc-Ge film under 260 mJ/cm$^2$, thermally annealed nc-Ge film at 350 °C and 450 °C.

### 3.2. Laser crystallization of a-Ge:H/SiN$_x$ multilayer

In order to achieve more controllable nc-Ge materials, we prepared nc-Ge/SiN$_x$ multilayers by laser crystallization of a-Ge:H/SiN$_x$ multilayers with a-Ge:H sublayer thickness values ranging from 4 nm to 10 nm. Figure 5 shows the cross-sectional TEM image of as-grown a-Ge:H/SiN$_x$ ML, in which the layered structures can be well identified. The thickness values of a-Ge:H and SiN$_x$ sublayer are 4.1 nm and 5.8 nm, respectively, which are in good accordance with the pre-designed values (4 nm/6 nm). Figure 6 gives the Raman spectra of laser-crystallized (170 mJ/cm$^2$) a-Ge:H/SiN$_x$ MLs with different values of Ge sublayer thickness. It is clearly shown that the a-Ge:H sublayer is crystallized and the corresponding crystallinity is estimated to be around 40%.

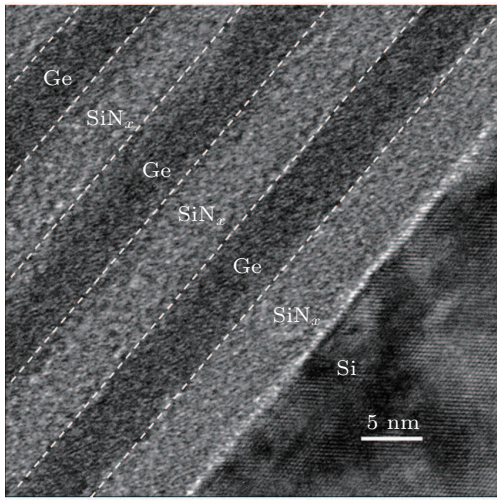



**Fig. 5.** The cross-section TEM image of as-grown a-Ge:H/SiN$_x$ (4 nm/6 nm) ML.

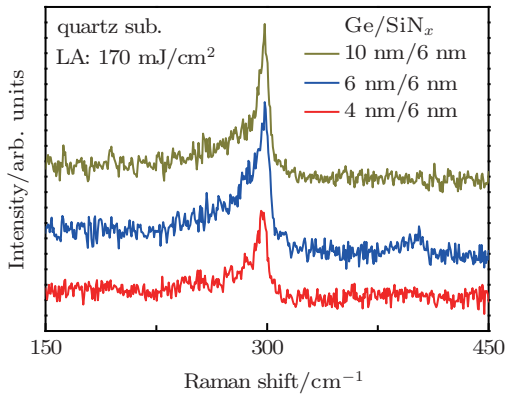



**Fig. 6.** (color online) Raman scattering spectra of MLs with some different values of Ge sub-layer thickness after LA under 170 mJ/cm$^2$.

The size, distribution, and crystal structure of prepared nc-Ge/SiN$_x$ (4 nm/6 nm) ML on quartz by laser annealing were further studied by planar-view TEM images. As shown in Fig. 7(a), it is found that the nanocrystals are randomly distributed and the density is estimated to be $\sim 1\times10^{11}$ cm$^{-2}$. Figure 7(b) shows a corresponding high-resolution TEM (HRTEM) image, where nanocrystalline Ge is well identified as marked by the white circles. The images in the inset of Fig. 7(b) clearly show lattice fringes, from which the interplanar spacings are evaluated to be 0.323 nm and 0.201 nm, corresponding to the {111} and {220} planes respectively. The spacing between nc-Ge is also estimated to be in a range of 2 nm–4 nm. A statistic size distribution of nanocrystals is plotted in Fig. 7(c), which indicates that the lateral size varies from 6 nm to 27 nm with an average of $\sim$ 14 nm.

We also estimated the optical band gap of laser crystallized nc-Ge/SiN$_x$ MLs. As shown in Table 1, the value of $E_{\rm opt}$ decreases from 0.83 eV to 0.70 eV when the Ge sub-layer thickness increases from 4 nm to 10 nm. The decrease of optical band gap may be ascribed to the following factors. One is the increase of crystallinity and the other is the formation of a two-dimensional system due to the confinement along the growth direction. Further studies are needed to clarify this point more clearly.

Figure 8 shows the temperature-dependent dark conductivities of nc-Ge/SiN$_x$ MLs. The room temperature conductivities are on the order of $10^{-2}$ S·cm$^{-1}$–$10^{-1}$ S·cm$^{-1}$, which are much higher than that of a-Ge:H ($9.2\times10^{-5}$ S·cm$^{-1}$) but about two orders of magnitude lower than that of laser annealed nc-Ge single layer under 100 mJ/cm$^2$ (2.3 S·cm$^{-1}$). With temperature increasing to 423 K, no prominent increase

of conductivity is observed for ML. Just like an nc-Ge single layer, conductivity is thermally activated and only a single conduction process is observed in nc-Ge/$SiN_x$ ML. The corresponding room temperature conductivity is plotted in the inset of Fig. 8 and the activation energy is listed in Table 1, which reveals that $E_a$ (0.04 eV $\sim$ 0.08 eV) is as small as that of an nc-Ge single layer. Hall measurements indicate that the major carriers of an nc-Ge/$SiN_x$ (10 nm/6 nm) ML are holes and the corresponding Hall mobility is 2.4 $cm^2 \cdot V^{-1} \cdot s^{-1}$ (Table 2), which is lower than that of an nc-Ge single layer.

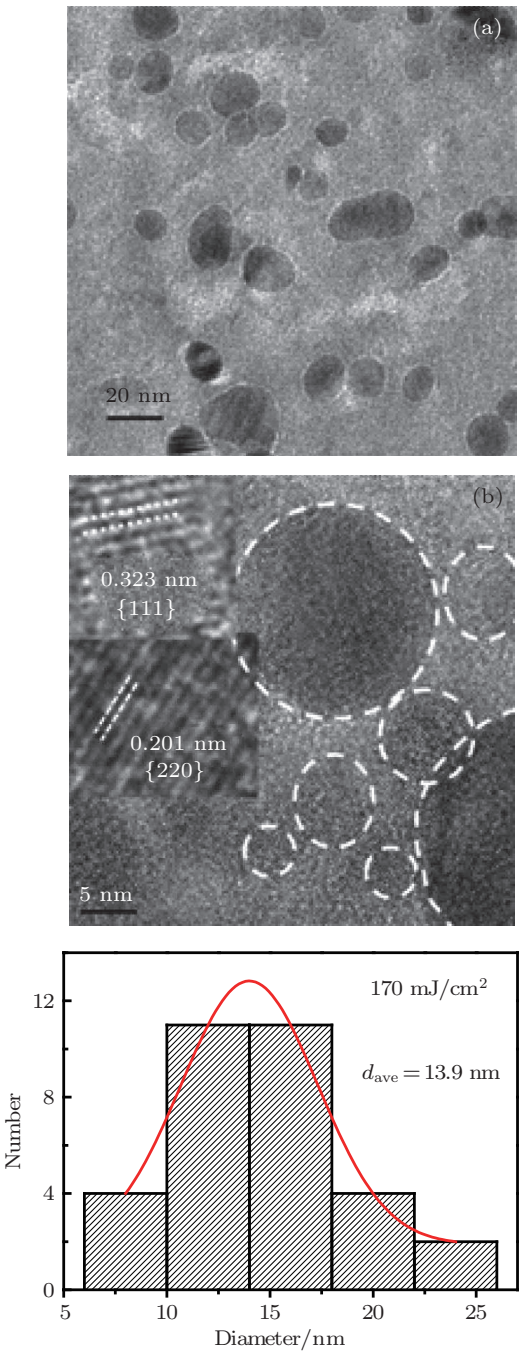



**Fig. 7.** (color online) Planar-view TEM images of laser crystallized nc-Ge/$SiN_x$ ML on quartz: (a) low resolution, (b) high resolution, and (c) a statistic distribution of crystal size. Circles in Fig.7(b) are marked to guide the eye, and the insets show the lattice fringes.

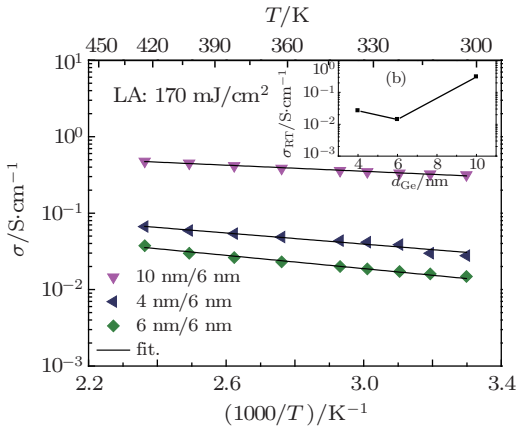



**Fig. 8.** (color online) Temperature-dependent dark conductivities of nc-Ge/$SiN_x$ MLs prepared by LA. The inset shows the corresponding room temperature conductivity.

**Table 2.** Hall measurements results of a-Ge:H, and nc-Ge films prepared by laser annealing: SL (260 mJ/cm$^2$) and ML (10 nm/6 nm, 170 mJ/cm$^2$).

| Sample | Conduction type | $\mu_H$/cm$^2$·V$^{-1}$·s$^{-1}$ |
|---|---|---|
| a-Ge:H | p | 0.11 |
| nc-Ge SL | p | 39.4 |
| nc-Ge/$SiN_x$ MLs | p | 2.4 |

From Table 1, it is found that the activation energy in a nc-Ge-based film is very small and close to each other, no matter whether the sample is single- or multi-layer, or it is prepared by LA or TA.[9] Fujii *et al.*[31] proposed that the activation energy in nc-Ge nanocrystals dispersed in $SiO_2$ matrix consists of two components: the electrostatic charging energy of particles ($E_C$) and the energy difference of confinement level ($\Delta E_d$) between the neighboring nanocrystals due to the grain size distribution. $E_C$ and $E_d$ are given as[31]

$$E_C = \frac{e^2}{4\pi\varepsilon\varepsilon_0 d}\frac{s/d}{0.5+s/d}, \tag{3}$$

$$E_d = A/d^2, \tag{4}$$

where $\varepsilon$ is the dielectric constant of material surrounding nc-Ge ($\approx$ 16), $\varepsilon_0$ is the permittivity in vacuum, $s$ is the distance between particles, $d$ is the average diameter of nc-Ge, and $A$ is the confinement constant dependent on the degree of confinement.[32] From the planar-view TEM images of our samples, $d$ varies from 6 nm to 27 nm with an average of 13.9 nm and $s$ is in a range of 2 nm–4 nm. Consequently, $E_C$ is no larger than 0.008 eV, which is one order of magnitude smaller than experimental $E_a$ value ($\sim$ 0.08 eV). In fact, the charging energy necessary to add a carrier to a nanocrystal is considerable at low temperature but negligible at our test temperature ($>$ 300 K). As for $\Delta E_d$, equal to $E_d(d_1) - E_d(d_2)$, it is estimated to be $\sim$ 0.03 eV even for strong three-dimensional confinement[32] based on the HRTEM observations, which is much lower than experimental $E_a$ value. Therefore, this model is not suitable for our sample. Zhang *et al.*[23] considered the activation energy $E_a = E_C + E_G$. Here, $E_C$ is the electron

charging energy mentioned above, and $E_G$ is the activation energy needed for the carrier generation which should be related to the Fermi level. It has been suggested that more surface states may exist on the surface of formed nc-Ge film which pin the Fermi level close to the valence band. By using surface passivation treatment, it will be helpful for depinning of Fermi level at Ge surface.[33] Due to the Fermi level pinning effect, the conduction activation energy is very small for nc-Ge film and the hole concentration is very high ($\sim 10^{18}$ cm$^{-3}$), which results in the weak temperature dependence of conductivity.

It is noticed that the mobility of the multilayered nc-Ge sample is lower than that of the nc-Ge single layered one. This can be explained by the smaller crystallinity and the different surrounding conditions of nc-Ge in multilayer. It is found that a higher laser fluence should be used to crystallize the a-Ge-based multilayer than to crystallize the a-Ge single layer. A laser fluence of 100 mJ/cm$^2$ is enough to crystallize an a-Ge single layer with a crystallinity about 46%. Meanwhile, the crystallinity of multilayers (6 nm/6 nm) is about 47% after 170 mJ/cm$^2$ laser annealing. Higher laser fluence can increase the crystallinity and improve the conductivity but may damage the multilayered structures[14] to result in broad size distribution. On the other hand, the carrier transport in multilayered structures may be strongly affected by the interfaces between nc-Ge and a-SiN$_x$ layers, which can also cause the low carrier mobility.

## 4. Conclusions

In this paper, the laser annealing technique is used to crystallize an a-Ge:H single layer and an a-Ge:H/SiN$_x$ multilayer to obtain nc-Ge films. The formation of nc-Ge is confirmed by Raman spectra and TEM observations, and its optical band gap is reduced compared with that of amorphous film. The carrier transport properties are systematically studied for both an nc-Ge single layer and an nc-Ge/SiN$_x$ multilayer. It is found that the transport process is dominated by the conduction through extended states in a-Ge:H film, whereas it is changed into the tunneling conduction process through nc-Ge for the laser crystallized sample. After the formation of nc-Ge, the Fermi level is pinned at the gap close to the valence band, which results in the p-type conduction characteristic of nc-Ge film as well as the very small conduction activation energy. Laser crystallization can also improve the crystalline quality which is reflected by the relatively high mobility. The Hall mobility is 39.4 cm$^2\cdot$V$^{-1}\cdot$s$^{-1}$ for nc-Ge single layer and 2.4 cm$^2\cdot$V$^{-1}\cdot$s$^{-1}$ for multilayer, which is significantly improved compared with their amorphous counterpart (0.11 cm$^2\cdot$V$^{-1}\cdot$s$^{-1}$). Our results demonstrate that the good-quality nc-Ge films can be prepared by laser annealing technique to avoid high temperature treatment, which can be potentially applied to Ge-based devices.

## References


[1] Poncet A, Souifi A, Baron T and Gautier E 2006 *Solid State Electron.* **50** 1310
[2] Tawancy H 2011 *Scr. Mater.* **65** 863
[3] Huang W, Liu J, Cai C, Lu Q, Liu S and Qin C 2010 *Chin. Phys. B.* **19** 097801
[4] Ortiz M, Rodriguez A, Sangrador J, Rodriguez T, Avella M, Jimenez J and Ballesteros C 2005 *Nanotechnology* **16** S197
[5] Xu H, Chan Y and Su L 2011 *Chin. Phys. B* **21** 107801
[6] Singha R, Manna S, Das S, Dhar A and Ray S 2010 *Appl. Phys. Lett.* **96** 233113
[7] Mitsui M, Arimoto K, Yamanaka J, Nakagawa K, Sawano K and Shiraki Y 2006 *Appl. Phys. Lett.* **89** 192102
[8] Kuo P, Chao T, Huang J and Lei T 2009 *IEEE Electron Dev. Lett.* **30** 234
[9] Li C, Xu J, Li W, Sun S, Jiang X and Chen K 2012 *J. Vac. Sci. Technol. B* **30** 051201
[10] Khan A, Mehmood M, Rana A and Muhammad T 2010 *Appl. Surf. Sci.* **256** 2031
[11] Wang Z, Wang J, Jeurgens L and Mittemeijer E 2008 *Phys. Rev. B* **77** 045424
[12] Knaepen W, Detavernier C, Van Meirhaeghe R, Sweet J and Lavoie C 2008 *Thin Solid Films* **516** 4946
[13] Santos P, Zanatta A, Dondeo F, Trampert A, Jahn U, Comedi D, Pudenzi M and Chambouleyron I 2001 *Journal of Non-Crystalline Solids* **299** 137
[14] Salihoglu O, Kurum U, Yaglioglu H, Elmali A and Aydinli A 2011 *J. Appl. Phys.* **109** 123108
[15] Salihoglu O, Kurum U, Yaglioglu H, Elmali A and Aydinli A 2012 *J. Vac. Sci. Technol. B* **30** 011807
[16] Watakabe H, Sameshima T, Kanno H and Miyao M 2006 *Thin Solid Films* **508** 315
[17] Mondal S and Ray S 2009 *Appl. Phys. Lett.* **94** 223119
[18] Poulsen P, Wang M, Xu J, Li W, Chen K, Wang G and Feng D 1998 *J. Appl. Phys.* **84** 3386
[19] Wang H, Lusquinos F and Yao Y 2012 *Appl. Phys. A* **107** 307
[20] Tsao C, Campbell P, Song D and Green M 2010 *J. Crystal Growth* **312** 2647
[21] Yu P and Cardona M 2001 *Fundamentals of Semiconductors: Physics and Materials Properties*, 3rd edn. (Berlin: Springer Press) pp. 269–273
[22] Tsao C, Wong J, Huang J, Campbell P, Song D and Green M 2011 *Appl. Phys. A* **102** 689
[23] Zhang B, Yao Y, Patterson R, Shrestha S, Green M and Conibeer G 2011 *Nanotechnology* **22** 125204
[24] Song C, Chen G, Xu J, Wang T, Sun H, Liu Y, Li W, Ma Z, Xu L, Huang X and Chen K 2009 *J. Appl. Phys.* **105** 054901
[25] Clark A 1967 *Phys. Rev.* **154** 750
[26] Giangregorio M, Losurdo M, Ambrico M, Capezzuto P, Bruno G and Tapfer L 2006 *J. Appl. Phys.* **99** 063511
[27] Tsai C, Yu S, Hsin C, Huang C, Wang C and Wu W 2012 *Crystal Eng. Comm.* **14** 53
[28] Chen G, Xu J, Xu W, Sun H, Mu W, Sun S, Ma Z, Huang X and Chen K 2012 *J. Appl. Phys.* **111** 094320
[29] Chen G, Song C, Xu J, Wang D, Xu L, Ma Z, Li W, Huang X and Chen K 2010 *Acta Phys. Sin.* **59** 5681 (in Chinese)
[30] Xu X, Grigoropoulos C and Russo R 1995 *J. Heat Transfer* **117** 708
[31] Fujii M, Mamezaki O, Hayashi S and Yamamoto K 1998 *J. Appl. Phys.* **83** 1507
[32] Barbagiovanni E, Lockwood D, Simpson P and Goncharova L 2012 *J. Appl. Phys.* **111** 034307
[33] Thathachary A, Bhat K, Bhat N and Hegde M 2010 *Appl. Phys. Lett.* **96** 152108